PHYSICAL REVIEW E **67**, 050702(R) (2003)

Annihilation of nematic point defects: Postcollision scenarios

Zlatko Bradač,[1] Samo Kralj,[1,2] Milan Svetec,[1,*] and Slobodan Žumer[3,2]
[1]*Laboratory of Physics of Complex Systems, Faculty of Education, University of Maribor, Koroška 160, 2000 Maribor, Slovenia*
[2]*Condensed Matter Physics Department, Jožef Stefan Institute, Jamova 39, 1000 Ljubljana, Slovenia*
[3]*Department of Physics, Faculty of Mathematics and Physics, University of Ljubljana, Jadranska 19, 1000 Ljubljana, Slovenia*
(Received 22 July 2002; published 21 May 2003)

We perform a study of the annihilation of a nematic radial and hyperbolic point defects with the main focus on the confinement induced collision and postcollision scenarios. Brownian molecular dynamics on a semimicroscopic lattice is used. Initially a pair of defects, separated for 1.4–1.7 radii, is induced at the axis of the cylindrical capillary. In such a configuration defects start to approach slowly. In the early stage, their cores are negligibly influenced by the mutual interaction. When the distance becomes comparable to the nematic correlation length, the cores significantly deform. In the collision regime, defects gradually merge. We observe two qualitatively different scenarios in the postcollision regime, depending on the degree of (meta) stability of the initially imposed escaped structure with point defects.

DOI: 10.1103/PhysRevE.67.050702 PACS number(s): 61.30.Cz, 61.72.Bb

The physics of defects [1] has been an attractive branch of research for years. It possesses many universalities and consequently involves different fields of physics ranging from the particle physics to cosmology [2]. A particularly suitable medium to study defects are uniaxial nematic liquid crystals (LCs) because of their simplicity, soft-liquid character, and optic transparency. These properties make them amenable to experimental observations [3,4].

Several attempts have been made to study the interaction between nematic radial and hyperbolic *point* (hedgehog) defects [1,5] bearing the topological charge $q=1$. Theoretically, there is a rather clear consensus about the core structure of these isolated defects [6–8] although an experimental confirmation of the theoretical predictions is still lacking. Also rather well explored [9–13] is the interaction between a pair radial-hyperbolic hedgehog in the precollision regime, where the cores of defects are negligibly affected by their mutual interaction. However, none of these studies focus on the exact behavior during the collision. In general collision, details can influence experimentally accessible macroscopic scale.

In order to understand the collision details we first review the core structure of isolated point defects with $q=1$. In the continuum approach their cores are commonly described using the traceless nematic tensor order parameter Q [6,14]. The essentially spherically symmetric and isotropic uniaxial defect core is expected only close to the isotropic-nematic phase transition and for limited range of anisotropy of the characteristic nematic elastic constants [14]. In a more general case the point defects broaden into a topologically equivalent ringlike structure [6,7,15]. In this structure the positive uniaxial ordering at the center of the defect is surrounded by the ring that undergoes a negative uniaxial ordering. The ring is further enclosed within the torus [8] exhibiting the maximal biaxiality. The size of the core [7,8] is roughly given by the relevant nematic order parameter correlation length (the uniaxial $\xi_n<20$ nm and the biaxial ξ_b $\sim$20 nm length for a pointlike and ringlike core structure, respectively). Note that because of these relatively small lengths the predicted core structures have not yet been verified experimentally.

The annihilation of nematic point defects has been most extensively studied in the cylindrical geometry [9–11] where the lateral surface walls enforce homeotropic (the molecules tend to be oriented along the surface normal) anchoring. So far all the studies have been focusing on the precollision regime. It has been shown that the defects annihilate into the defectless state, if their separation d is less than the diameter of the cylinder [11,16]. Experimental measurements [9] further suggest that the relative velocity of close enough defects is roughly proportional to $1/d$ and that the motion of the defects is strongly anisotropic.

In this paper we present the study of the postcollision evolution of collided nematic radial and hyperbolic hedgehog using the semimicroscopic approach. The dynamics of the system is studied with the orientational Brownian molecular dynamics enabling us to access macroscopic time scales. Consequently, we can study both postcollision and precollision stages. We further distinguish between two qualitatively different postcollision scenarios. In the first case the defects annihilate into the defectless state. In the second case the collided defects trigger the transition from the initially metastable to the globally stable nematic structure characterized by two line defects.

I. MODEL INTERACTION

In our semimicroscopic approach *molecules* interact via a generalized van der Waals pairwise interaction, which to some extent takes into account elastic anisotropy of nematic LCs. The interaction of a pair of rodlike LC molecules at $\vec{r}_i$ and $\vec{r}_j=\vec{r}_i+\vec{\Delta}r$, oriented along $\vec{e}_i(\vec{r}_i)$ and $\vec{e}_j(\vec{r}_j)$, is expressed as [17]

$$V_{ij}=-\frac{J}{\Delta r^6}\left(\vec{e}_i\cdot\vec{e}_j-\frac{3\varepsilon}{\Delta r^2}(\vec{e}_i\cdot\vec{\Delta r})(\vec{e}_j\cdot\vec{\Delta r})\right)^2. \quad (1)$$

*Present address: Regional Development Agency, Mura Ltd., Lendavska 5A, 9000 Murska Sobota, Slovenia

The quantity J is a positive interaction constant and ε measures the degree of orientational anisotropy. For $\varepsilon=0$ the isotropic Maier-Saupe (also called Lebwohl-Lasher [18]) and for $\varepsilon=1$ the induced dipole-induced dipole-type interaction [17] is obtained. This model reasonably describes properties of nematic LCs for $\varepsilon<0.3$. In the continuum description, the $\varepsilon=0$ case roughly corresponds to the Frank uniaxial description in the so called equal elastic constant approximation [4]. For $\varepsilon\neq 0$ the degeneracy between the Frank elastic constants is partially lifted [17]. Note that the term molecule in our description stands for a cluster of (real) molecules. The cluster size is somewhere between 1 and the number of molecular sites within a sphere that includes also the first neighboring molecules of the lattice [19,16].

II. PARAMETRIZATION

The local orientation of the ith molecule in the laboratory frame is parametrized as $\vec{e}_i=\vec{e}_x\sin\Theta\cos\Phi+\vec{e}_y\sin\Theta\sin\Phi+\vec{e}_z\cos\Theta$, where the angles $\Theta=\Theta(\vec{r}_i,t)$ and $\Phi=\Phi(\vec{r}_i,t)$ are the variational parameters. They are given at a discrete time t and position $\vec{r}_i=(x_i,y_i,z_i)$ in the Cartesian coordinate system oriented along the unit vectors $\vec{e}_x$, $\vec{e}_y$ and $\vec{e}_z$. Molecules are allowed to wander around the points of the three-dimensional hexagonal lattice with spacing a_0. By such a box restricted dynamics [16] we get rid of the lattice induced ordering anisotropy known to appear in regular lattices.

III. DYNAMICS

The Brownian molecular dynamics method is used to follow the rotational dynamics of the system [20]. At each time interval Δt (one sweep) the molecular orientation of the system is updated in the local frame using [20,16]

$$\psi^{(l)}(\vec{r}_i,t+\Delta t)=\psi^{(l)}(\vec{r}_i,t)-\sum_{j\neq i}\frac{D_{ij}^{(l)}}{kT}\Delta t\frac{\partial V_{ij}}{\partial\psi^{(l)}}+\psi_{r,i}^{(l)}, \quad (2)$$

where ψ stands either for Θ or Φ and the superscript (l) indicates the local molecular frame in which the rotation diffusion tensor $D_{ij}^{(l)}$ is diagonal. In calculations its eigenvalues are assumed to be degenerated and equal to D. The quantity k is the Boltzmann constant, T is the temperature, and $\Theta_{r,i}^{(l)}$ and $\Phi_{r,i}^{(l)}$ are stohastic variables obeying the Gaussian distribution. The probabilities are centered at $\Theta_{r,i}^{(l)}=0$ and $\Phi_{r,i}^{(l)}=0$. The width of the distribution is proportional to $\sqrt{T}$. The corresponding multiplicative constant is chosen so as to yield a correct equilibrium value of the nematic uniaxial order parameter. The summation in Eq. (2) is limited to neighbors within a sphere of a radius $2a_0$ [16].

The shortest time interval Δt of the model in the simulation is set by $\Delta t D\sim 0.01$. For a typical nematic LC this ranges within the interval $\Delta t\sim 0.001$ μs to $\Delta t\sim 0.1$ μs depending on the size of a molecule. An estimate of a Δt value was obtained by comparing a response of the system to an external perturbation calculated from the semimicroscopic and the continuum type approach [16].

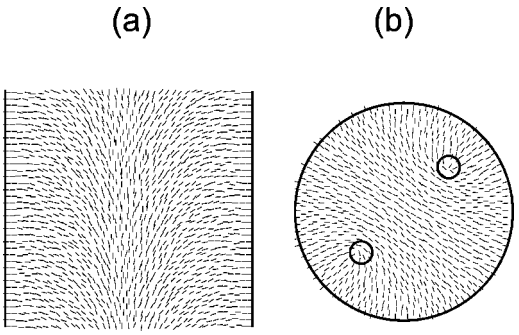

FIG. 1. The (a) escaped (E) structure and (b) planar (P) structure with line defects in the director field $\vec{n}$ representation. The structures are presented in the (x,z) and (x,y) planes, respectively. In (b) the line defects of strength 1/2 are indicated by small circles. The cylinder wall is described with a full line.

IV. GEOMETRY

Our system is confined to a cylindrical cavity of radius $R=N_r a_0$ and length $L=N_z a_0$. The integers $2N_r$, N_z are typically chosen between 40 and 80. The cylinder axis is set along the z direction of the laboratory coordinate system. The lateral surface strongly enforces the neighboring molecules orientation along the surface normal, corresponding to the strong homeotropic anchoring [4]. At a distance L along the cylinder axis, periodic boundary conditions are imposed simulating an infinite cylindrical capillary.

The equilibrium nematic director configurations of our system [16] are topologically equivalent *escaped* (E) structure or *planar* (P) *structure with line defects* shown in Fig. 1. For radii above the critical value $R_c(\varepsilon)$ the E structure is stable and the P structure for $R<R_c(\varepsilon)$. The value of $R_c(\varepsilon)$ monotonically increases with ε ($R_c(0)\sim 16a_0$, and $R_c(0.07)\sim 25a_0$ [16]). In the E structure [Fig. 1(a)] on approaching the cylinder axis radially the molecules gradually reorient ("escape") from the radial orientation at the wall towards $\vec{e}_z$ (schematically: $>>>$) or equivalently $-\vec{e}_z$ ($<<<$) at the cylinder axis. In the P structure [Fig. 1(b)] the molecules are constrained to the azimuthal (x,y) plane. Close to the cylinder axis molecules are preferentially aligned along a symmetry breaking direction. In order to fullfil the strong homeotropic anchoring at the cylinder wall, two line defects of the strength 1/2 parallel to the cylinder axis are formed.

V. PRECOLLISION REGIME

In the simulation we initially placed the radial and the hyperbolic hedgehog on the cylinder axis. This was achieved by enforcing three alternatively oriented escaped domains (i.e., $>>><<<>>>$) by using the analytic ansatz [11]. The initial separation of defects is close enough so that the interaction between defects is sufficiently strong [i.e., $d_0/(2R)=0.7<1$, obtained for $d=d_0\equiv 35a_0$ and $2N_r=50$]. For such initial conditions, the collision of defects and further evolution into the final equilibrium structure are reached in a computationally accessible time ($\sim 10\,000$ sweeps). On the other hand, the separation is large enough so that the cores of defects reach their quasiequilibrium configuration

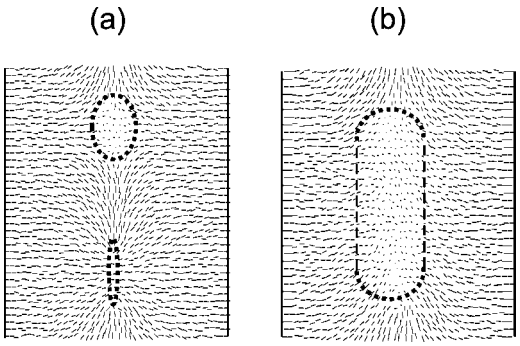

FIG. 2. Different annihilation stages of a pair of nematic defects. The snapshots of structures, resembling the $\vec{n}$ representation, are shown in the (x,z) plane. A point indicates a *molecule* oriented out of the plane. (a) The structure with the two rings after 2000 sweeps (left, radial; right, hyperbolic hedgehog). The rings are denoted with dotted lines. In the case shown, the rings are caught at approximately perpendicular relative orientation. (b) Soon after the collision the collided defects form a single ring. The ring part that closely resembles the *P*-like profile is denoted with dashed line. The simulation is run for $2N_r=50$, $N_z=80$, $\epsilon=0$. After 7800 sweeps the *E* profile is reached, shown in Fig. 1(a). The simulation for $\epsilon=0.07$, for which $R_c(\varepsilon)>R$, exhibits qualitatively similar stages, but the nucleus created in the ring collision grows and drives the system into the *P* structure. The cylinder wall is denoted with a full line.

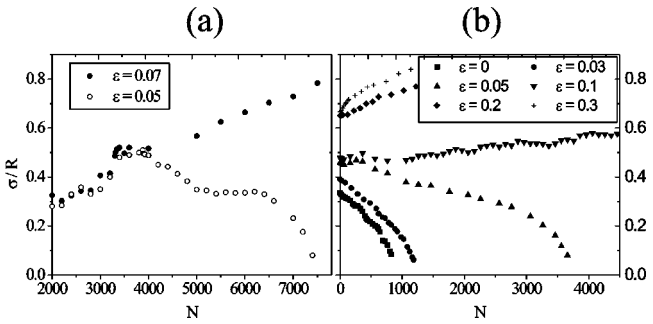

FIG. 3. The ring radii time evolution of the annihilation (open circles) and nucleation (full circles) process. *N* counts the sweeps in the simulation. The two scenarios shown correspond to the cases $\varepsilon=\varepsilon_c\pm0.01$, where $\varepsilon_c=0.06$ stands for the critical value of ε for a constant radius, separating two qualitatively different postcollision scenarios. (b) Postcollision regime: the ring radius as a function of time and ϵ. The upper three curves describe nucleation and the remaining ones the annihilation process. In (b) the sweeps are counted after the collision of defects. Note that the collision time t_c and the precollision ring radii sizes strongly depend on ε. $\sigma=\xi_r^{(-)}+\xi_r^{(+)}$ and $\sigma=2\xi_r$ in the precollision and postcollision regimes, respectively. In all cases $2N_r=50$ and $N_z=80$.

before being apparently influenced by each other [11]. Some important stages of annihilation, calculated for $\varepsilon=0$, are shown in Fig. 2. We initially enforce a pointlike defect. After some 2000 sweeps [Fig. 2(a)] the defects adopt the ringlike core structure, as the continuum theory predicts [7,8]. The points belonging to the ring correspond to the largest connected local distortions in nematic ordering within the core of defect. In the continuum Q-tensor representation on crossing the ring the exchange of Q eigenvalues takes place [6]. To describe the time evolution of rings we introduce the diameters $2\xi_r^{(+)}$ and $2\xi_r^{(-)}$, measuring the largest ring diameter of the radial and the hyperbolic hedgehog, respectively. The ring radii appear to be equal for $\varepsilon=0$ in accordance with the prediction of the elastic theory [21]. In our simulation the equilibrium ring radius is $\xi_r^{(\pm)}\sim7a_0$. With $\varepsilon\neq0$ this degeneracy is lifted and the core of the radial hedgehog defect becomes apparently relatively larger for $\varepsilon>0.1$. Due to confinement the rings after the creation tend to orient with their axes perpendicular to the cylinder axis [22] [Fig. 2(a)], breaking the cylindrical symmetry of the structure. This symmetry was commonly assumed in previous studies [23].

In Fig. 3(a) we follow the time variation of the sizes of rings after they attain their equilibrium value. In the regime where $d(t)>\xi_{eq}^{(\pm)}$, where the subscript eq denotes the equilibrium ring radius size, the defects can be well distinguished and the ring radii are constant within the experimental error. The two rings gradually attract each other and their axes slowly (on the time scale of 1000 sweeps) rotate due to fluctuations. From the simulation we conclude $d(t)\sim(t_c-t)^{0.5\pm0.2}$, where $t_c=t_c(\varepsilon)$ stands for the ''collision time,'' which agrees with available experimental observations [9].

We refer to this stage as the *precollision* regime.

VI. COLLISION REGIME

When $d\sim\xi_{eq}^{(\pm)}$ ($\approx$6500 sweeps for $\varepsilon=0$) the core structure of defects become influenced by each other and the ring radii gradually increase with time: the collision regime is entered. Then the rings touch and merge into a single combined ring [Fig. 2(b)], described by ξ_r, with generally twisted structure. This is due to the fact that prior to collision the relative orientation of ring axes are rather arbitrary. In this event the escapedlike character of the structure between defects, which was responsible for the topological stability of defects, vanishes. The defects now merge to the extent that they are indistinguishable after entering the postcollision regime.

VII. POSTCOLLISION REGIME

We observe two qualitatively different postcollision scenarios depending on the cylinder size. For $R>R_c(\varepsilon)$ the collided defects decay into the defectless *E* structure [Fig. 1(a)]. For $\epsilon=0$ the ''combined ring'' disappears after 7500 sweeps and the equilibrium structure is reached in $\approx$7800 sweeps. A decay into a defectless state for different anisotropies ϵ is shown in Fig. 3(b). In the decay process the shrinking of the defect structure (due to the ''pressure'' resulting from different free energy densities in the system) is accompanied by decreasing the twist of the ring in order to decrease the effective curvature of the ring. The interplay of these driving forces yield commonly a three-stage $\xi_r(t)$ dependence. At the end of the first stage, the ring untwists and becomes circular at the end of the second stage. In the third stage, the shrinking circular ring gradually disappears. The relative orientation of ring axes at the collision seems not to affect significantly the annihilation time.

For $R \lesssim R_c(\varepsilon)$ instead of the annihilation into the defectless structure, the collided defects trigger the structural transition into the *planar* structure. The reason behind this is the fact that for $R \lesssim R_c(\varepsilon)$ the *E* structure, which closely resembles the initial nematic structure of our simulation (the ''domains'' outside the defects have the *E*-like structure), is metastable with respect to the *P* one. Note also that the cores of isolated defects exhibit locally *P*-like configuration. These *P*-like ''nuclei'' of well separated defects are too small to drive the whole system into the *P* structure. But in the collision a large enough ''nucleus'' is formed to trigger the transition. The growth (see Fig. 3) typically evolves in two stages. In the first stage the nucleus growth is three dimensional (radial and along the *z* axis). In the second stage, the separation between already pronounced line defects becomes saturated and the *P*-nucleus expansion now proceeds only along the cylinder axis. The velocity of the domain wall propagation along the *z* axis is determined by the free energy difference of the competing structures at the opposite sides of the wall. Consequently, ξ_r grows linearly with time. For $R \ll R_c(\varepsilon)$ each defect separately triggers the nucleation growth into the *P* structure. In this case the nucleation growth starts immediately and the centers of defects are not set into the relative motion. Note that in Fig. 3 we were changing the value of $R_c(\varepsilon)$ by varying ε and keeping R constant.

VIII. SUMMARY

We have studied the dynamics of the interacting pair nematic radial and hyperbolic hedgehogs. The Brownian molecular dynamics approach allowed us to monitor both, the precollision and the postcollision stage. Our results in the precollision regime are in accordance with known results that were obtained in the Frank-type continuum description (structure of defects [7,15,8], their relative size [21], and relative velocity of approaching defects). We, however, do not reproduce large anisotropy in the velocity of defects which seems to be due to backflow effects [12,13], which are not accounted here. In the collision the defects' core structures strongly overlap and gradually become indistinguishable. We observed two qualitatively different postcollision scenarios. For $R > R_c(\varepsilon)$ the defectless (i.e., vacuum) state is reached. For $R \lesssim R_c(\varepsilon)$ the collided cores of defect form a large enough nucleus of the stable phase in the metastable background to overcome the energy barrier separating the two phases. The anisotropy ε plays an important role in the simulation. For $\varepsilon > 0$ the rings of defects become different and consequently also their velocity. In addition, ε strongly influences the value of $R_c(\varepsilon)$. Note that the typical time scales of the precollision and postcollision regimes are expected to be drastically different in a large enough cavity (in comparison to the relevant nematic order parameter correlation length ξ). The precollision dynamics is governed by the nematic director field, whose characteristic relaxation time scales τ as $\tau \propto R^2$ [4]. By contrast the postcollision annihilation dynamics is governed by the nematic order parameter and consequently $\tau \propto \xi^2$ [22]. In our simulation, R (it ranges between 0.5 and 5 μm) and ξ and therefore also the time scales in both regimes are comparable.

This research was supported by the ESF network project COSLAB. We thank E.G. Virga, T.J. Sluckin, and H. Brand for stimulating discussion and comments.

[1] N.D. Mermin, Rev. Mod. Phys. **51**, 591 (1976).
[2] See http://theory.ic.ac.uk/coslab
[3] M.V. Kurik and O.D. Lavrentovich, Usp. Fiz. Nauk **154**, 381 (1988) [Sov. Phys. Usp. **31**, 196 (1988)], and references therein.
[4] P. G. de Gennes and J. Prost, *The Physics of Liquid Crystals* (Oxford University Press, Oxford, 1993).
[5] O.D. Lavrentovich, Liq. Cryst. **24**, 117 (1998).
[6] N. Schopohl and T.J. Sluckin, Phys. Rev. Lett. **59**, 2582 (1987).
[7] E. Penzenstadler and H.R. Trebin, J. Phys. (France) **50**, 1025 (1989).
[8] S. Kralj, E.G. Virga, and S. Žumer, Phys. Rev. E **60**, 1858 (1999); J. Phys. A **34**, 829 (2001).
[9] A.N. Pargellis, N. Turok, and B. Yurke, Phys. Rev. Lett. **67**, 1570 (1991).
[10] L.M. Pismen and B.Y. Rubinstein, Phys. Rev. Lett. **69**, 96 (1992).
[11] G.G. Peroli and E.G. Virga, Phys. Rev. E **59**, 3027 (1999).
[12] G. Toth, C. Denniston, and J.M. Yeomans, Phys. Rev. Lett. **88**, 105504 (2002).
[13] D. Svenšek and S. Žumer, Phys. Rev. E **66**, 021712 (2002).
[14] R. Rosso and E.G. Virga, J. Phys. A **29**, 4247 (1996); E.C. Gartland and S. Mkaddem, Phys. Rev. E **59**, 563 (1999).
[15] O.D. Lavrentovich, T. Ishikawa, and E.M. Terentjev, Mol. Cryst. Liq. Cryst. **299**, 301 (1997).
[16] Z. Bradač, S. Kralj, and S. Žumer, Phys. Rev. E **58**, 7447 (1998); **65**, 021705 (2002).
[17] G. Barbero, Mol. Cryst. Liq. Cryst. **195**, 199 (1991).
[18] P.A. Lebwohl and G. Lasher, Phys. Rev. A **6**, 426 (1972).
[19] C. Chiccoli, P. Pasini, F. Semeria, E. Berggren, and C. Zannoni, Mol. Cryst. Liq. Cryst. **290**, 237 (1996).
[20] D.L. Ermak, J. Chem. Phys. **62**, 4189 (1975).
[21] T.C. Lubensky, D. Pettey, N. Currier, and H. Stark, Phys. Rev. E **57**, 610 (1998).
[22] E.G. Virga and A. Sonnet (private communication).
[23] E.G. Virga and S. Kralj (unpublished).